

RESEARCH ARTICLE

10.1002/2016GC006624

Special Section:

Wilson Cycles and the Formation of Marginal Basins: Rifting Dynamics and Mantle Evolution from Mid-ocean Ridge Creation to Extinction

Key Points:

- Filtered directional derivatives of gravity reveal deeply buried fracture zones
- We present a new tectonic map of the West Somali Basin
- The Davie Fracture Zone is reinterpreted as an ocean-ocean fracture zone

Supporting Information:

- Supporting Information S1

Correspondence to:

J. J. J. Phethean,
j.j.j.phethean@durham.ac.uk

Citation:

Phethean, JJJ, LM Kalnins, J van Hunen, PG Biffi, RJ Davies, and KJW McCaffrey. (2016), Madagascar's escape from Africa: A high-resolution plate reconstruction for the Western Somali Basin and implications for supercontinent dispersal, *Geochem. Geophys. Geosyst.*, 17, 5036–5055, doi:10.1002/2016GC006624.

Received 1 SEP 2016

Accepted 5 DEC 2016

Accepted article online 20 DEC 2016

Published online 29 DEC 2016

Madagascar's escape from Africa: A high-resolution plate reconstruction for the Western Somali Basin and implications for supercontinent dispersal

Jordan J.J. Phethean ¹, Lara M. Kalnins ^{1,2}, Jeroen van Hunen ¹, Paolo G. Biffi ³, Richard J. Davies ⁴, and Ken J.W. McCaffrey ¹

¹Department of Earth Sciences, Durham University, Durham, UK, ²School of GeoSciences, University of Edinburgh, Edinburgh, UK, ³S.G.E.G. ENI, Milan, Italy, ⁴School of Civil Engineering and Geosciences, Newcastle University, Newcastle upon Tyne, UK

Abstract Accurate reconstructions of the dispersal of supercontinent blocks are essential for testing continental breakup models. Here, we provide a new plate tectonic reconstruction of the opening of the Western Somali Basin during the breakup of East and West Gondwana. The model is constrained by a new comprehensive set of spreading lineaments, detected in this heavily sedimented basin using a novel technique based on directional derivatives of free-air gravity anomalies. Vertical gravity gradient and free-air gravity anomaly maps also enable the detection of extinct mid-ocean ridge segments, which can be directly compared to several previous ocean magnetic anomaly interpretations of the Western Somali Basin. The best matching interpretations have basin symmetry around the M0 anomaly; these are then used to temporally constrain our plate tectonic reconstruction. The reconstruction supports a tight fit for Gondwana fragments prior to breakup, and predicts that the continent-ocean transform margin lies along the Rovuma Basin, not along the Davie Fracture Zone (DFZ) as commonly thought. According to our reconstruction, the DFZ represents a major ocean-ocean fracture zone formed by the coalescence of several smaller fracture zones during evolving plate motions as Madagascar drifted southwards, and offshore Tanzania is an obliquely rifted, rather than transform, margin. New seismic reflection evidence for oceanic crust inboard of the DFZ strongly supports these conclusions. Our results provide important new constraints on the still enigmatic driving mechanism of continental rifting, the nature of the lithosphere in the Western Somali Basin, and its resource potential.

1. Introduction

Continental breakup is a fundamental, but poorly understood, part of the plate tectonic cycle. Our understanding of the conditions needed for successful rift formation is particularly limited. Besides preexisting weak zones [Ziegler and Cloetingh, 2004] and thermal weakening due to rifting-related magmatism [Buck, 2007], it has also recently been shown that oblique rifting is an important mechanism in facilitating breakup [Brune *et al.*, 2012]. To further investigate these concepts, accurate reconstructions of rifting events with high spatial resolution are essential to enable detailed comparisons between models and observations [Nance and Murphy, 2013]. Detailed history of rifted margin evolution is also key in hydrocarbon exploration by enabling the prediction of the petroleum potential for conjugate basins with similar tectonostratigraphic histories [Beglinger *et al.*, 2012]. Some of the most significant rifting episodes in Earth's history occurred during supercontinent breakup, e.g., rifting between East and West Gondwana, which spanned many of our present-day continents.

Gondwana was assembled between 600 and 500 Ma in the Pan-African orogeny [e.g., Trompette, 2000; Van Hinsbergen *et al.*, 2011]. Beginning in the Jurassic, the subsequent breakup of East and West Gondwana carried Madagascar approximately southward, as shown by ocean magnetic anomalies [Ségoufin and Patriat, 1980; Rabinowitz *et al.*, 1983; Cochran, 1988; Eagles and König, 2008; Davis *et al.*, 2016], forming the Western Somali Basin (WSB) [Coffin and Rabinowitz, 1987; Geiger *et al.*, 2004]. Knowledge of Madagascar's former position within Gondwana, and the path it followed during its southward drift, is crucial for creating accurate plate tectonic reconstructions of Gondwana's dispersal.

Paleogeographic reconstructions of Madagascar's position in Africa (Figure 1) have a large range of fits, suggesting significantly different locations for the continent-ocean transition. This is primarily due to the lack of fracture zone expressions in bathymetry data, where the characteristic fracture zone topography is commonly obscured by over 5 km of sediment [Coffin *et al.*, 1986]. The Davie Fracture Zone (DFZ), commonly assumed to form the western transform fault [Coffin *et al.*, 1986] or continent-ocean transform margin [e.g., Gaina *et al.*, 2013] of the WSB, is one of the few fracture zones confidently identified. However, the DFZ is overlapped by several independently generated reconstructions [e.g., Smith and Hallam, 1970; Lottes and Rowley, 1990; Reeves, 2014]. This puts our understanding of this feature into doubt, and highlights the need for the comprehensive detection of fracture zones to support plate tectonic reconstructions of the basin.

In this paper, we present a detailed and self-consistent plate tectonic reconstruction of the WSB that can be used to further our understanding of the dynamics of continental breakup. We use a novel combination of free-air gravity, vertical gravity gradient, and filtered free-air gravity directional derivatives to determine the location of the extinct mid-ocean ridge (MOR) segments and map out a comprehensive set of gravity lineaments related to fracture zones in the WSB. Using global gravity data sets with 1 arc-minute resolution captures the complexity of the breakup geometry and motion, beyond what can be seen in widely spaced shipboard magnetic profiles, and also constrains the history of the basin to the west of 43°E where no magnetic anomaly identifications are available [e.g., Davis *et al.*, 2016]. These spreading-related features are tested against existing magnetic and seismic reflection data before being used to produce a high-resolution plate tectonic reconstruction.

The model provides new insight into Madagascar's position in Africa prior to Gondwana breakup, the nature of the DFZ, and the geometry and structure of the East African continental margin. This provides a significant advance toward a more comprehensive understanding of the nature of the margins and underlying lithosphere of the WSB, as well as a broader understanding of rifting events and continental breakup mechanisms.

2. Data and Processing

In this study, we used the distribution and orientation of fracture zones (FZs) and extinct MORs to construct a plate tectonic model for the WSB. These tectonic features were detected using a combination of gravity, magnetic, and seismic data.

2.1. Gravity Data

We used version 23 of the Sandwell and Smith gravity model [Sandwell *et al.*, 2014], which now has an accuracy of ~2 mGal (compared to 3–5 mGal in previous versions) following the addition of retracked CryoSat-2 and Jason-1 satellite altimetry data. This improvement allows detection of many buried structures, particularly short wavelength features such as extinct MORs and FZs [e.g., Sandwell *et al.*, 2014]. In addition to the widely-used free-air gravity anomaly, gradients such as the vertical gravity gradient (VGG) amplify short wavelength gravity signals, aiding the detection of relatively small features such as seamounts and ocean spreading structures [e.g., Kim and Wessel, 2011].

FZs are the inactive extensions of transform faults along the MOR, which run parallel to the spreading direction during their formation and therefore record plate motions. Oceanic plate ages, and thus seafloor depths, are offset across transform faults, causing a distinct bathymetric feature, which is permanently locked in by welding at ridge-transform intersections [Sandwell, 1984]. Variations in crustal thickness due to melt supply [Blackman and Forsyth, 1991; Gente *et al.*, 1995], transpression or transtension [Menard and Atwater, 1969], and thermal contraction [Collette, 1974] can also result in bathymetric expressions along fracture zones. The resulting linear ridges and troughs can be traced in bathymetric data in order to track the spreading history, which in turn may be used in constructing a plate tectonic model.

In heavily sedimented regions, however, spreading features may be completely buried. Fortunately, expressions of the spreading features are also preserved in gravity data, even when buried by sediments, due to lateral density contrasts between sediment, crust, and mantle across the structures. Gravity data therefore allows the derivation of paleospreading directions in heavily sedimented regions of the ocean [Sandwell *et al.*, 2014].

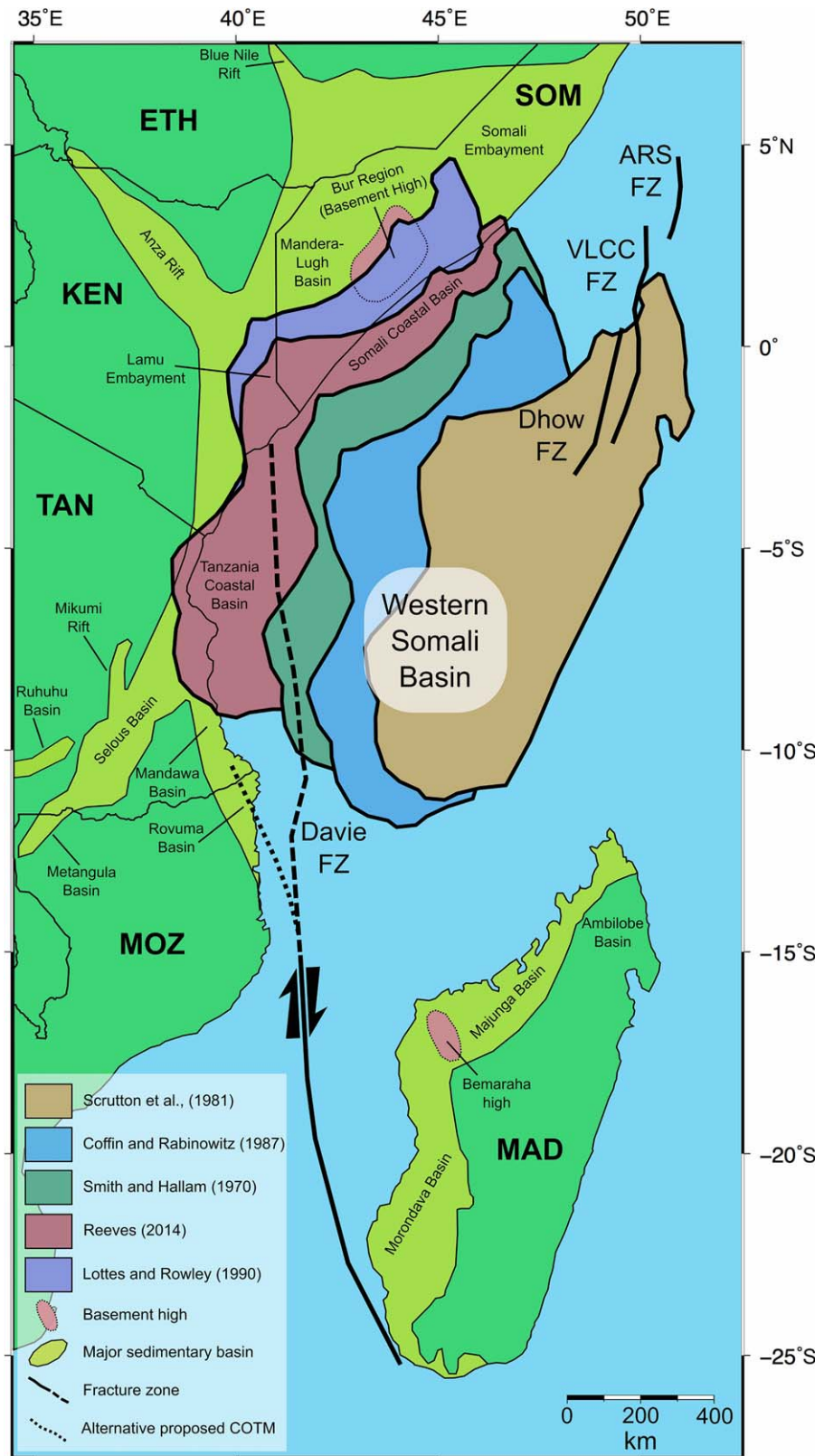


Figure 1. Published reconstructions for Madagascar’s paleoposition in Africa are shown alongside major continental basins, basement highs, and previously identified oceanic fracture zones. ARS, Auxiliary Rescue and Salvage; VLCC, Very Large Crude Carrier; ETH, Ethiopia; KEN, Kenya; MAD, Madagascar; MOZ, Mozambique; SOM, Somalia; TAN, Tanzania; COTM, Continent-ocean transform margin.

2.1.1. Bandpass Filtering and Gravity Gradients

We used a combination of directional derivatives and band-pass filtering to further enhance the portion of the gravity field associated with FZs. First, a Gaussian band-pass filter was used to remove short wavelength noise and shallow features within the sediment layer, together with long wavelength signals from deep mantle heterogeneities. *Mulder and Collette* [1984] found that most FZs produce anomalies with intermediate wavelengths between 50 and 200 km. We further refined these bounds empirically, looking for sharp, continuous linear anomalies parallel to the overall spreading direction derived from ocean magnetic anomalies, and found that wavelengths of 55–85 km best highlighted fracture zone structure.

After filtering, we exploited the linear nature of spreading features by taking directional gradients of the free-air gravity to emphasize lineations of a given orientation [e.g., *Mitchell and Park*, 2014]. This procedure has similar advantages to illuminating a topographic map to highlight fault scarps [e.g., *Arrowsmith and Zielke*, 2009]. In the case of the WSB, the ocean magnetic anomalies indicate an approximately N-S spreading direction. Therefore gradients taken along this strike would highlight spreading-perpendicular features, such as MOR segments, and those taken with an E-W strike would highlight spreading-parallel features, such as FZs. To account for local variability and changes in spreading direction, we took the directional gradient at 10° intervals between 30° clockwise and anti-clockwise of the chosen azimuth. This allowed near-perpendicular gradients to be sampled at all points along curved lineations, ensuring an unbiased sampling of the greatest gradient magnitudes. Examples showing the effect of changing the orientation and range of gradient sampling are provided in the supplementary material.

2.1.2. Testing the Detection Method

To check our methodology's usefulness in detecting spreading-related structures in buried oceanic crust, we tested it on a region of the Cape Basin, offshore South Africa (Figure 2a). Like the WSB, this basin has a

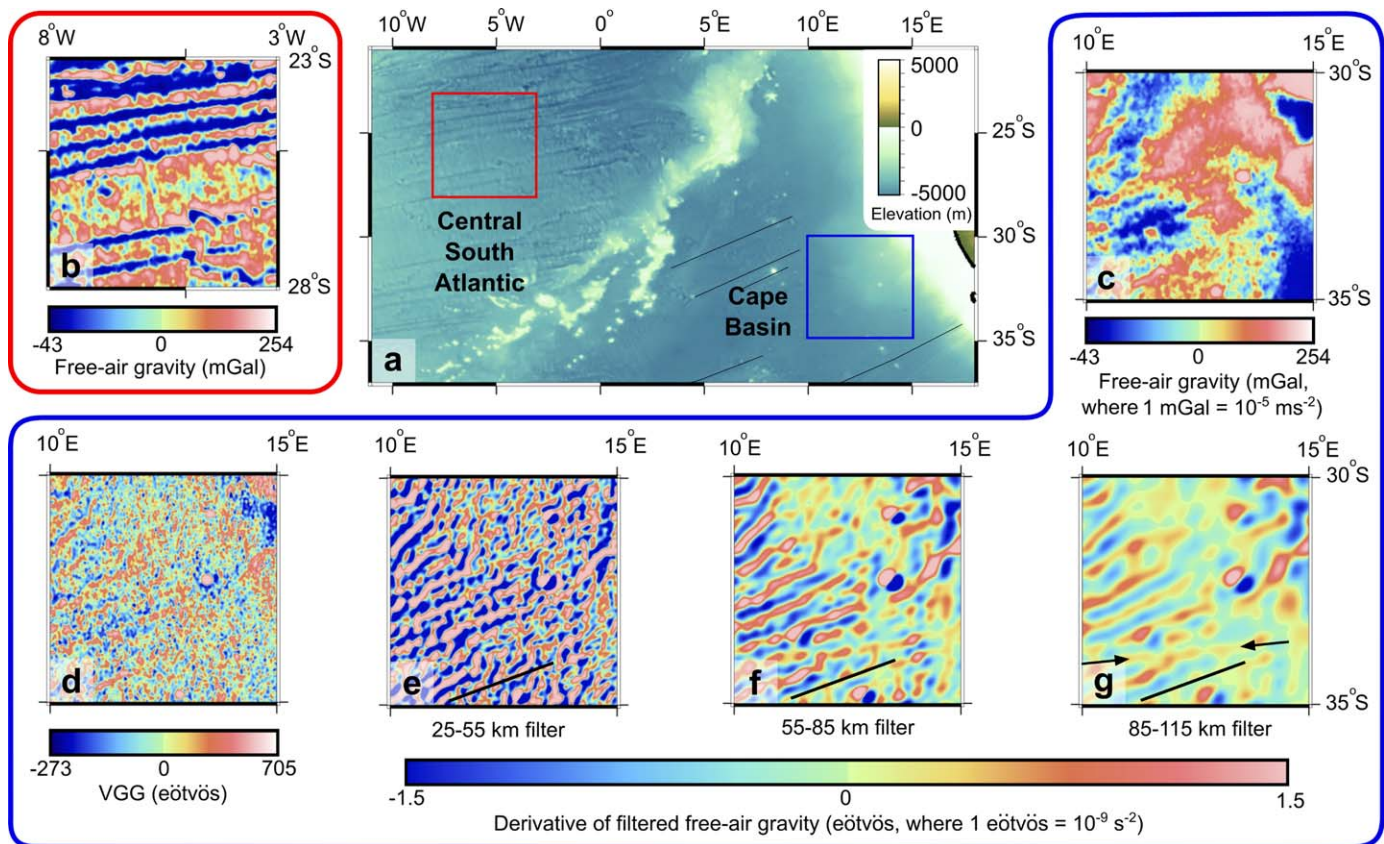


Figure 2. (a) Test location for the processing technique within the heavily sedimented Cape Basin, and an unsedimented example location in the Central South Atlantic. Major fracture zones of the Cape basin are marked as thin black lines. (b) Free-air gravity example of unsedimented Central Atlantic spreading features. (c) Free-air gravity from the heavily sedimented test location. (d) VGG from the test location. (e–g) Spreading-parallel derivatives of gravity after filtering to retain specified wavelengths. Black lines indicate spreading direction as constrained by major FZs from elsewhere in the Cape Basin; arrows in Figure 2g indicate merged anomaly lineations.

thick sedimentary cover (2–5+ km), resulting in enigmatic spreading features that are difficult to interpret from free-air gravity and VGG alone. The overall spreading rate is also similar to the WSB [e.g., *Eagles*, 2007], likely resulting in similar FZ morphology, and thus making this a very good natural laboratory. The free-air gravity anomaly of the test region within the Cape Basin was compared to that of an unsedimented example location from the Central Atlantic (Figures 2b and 2c), demonstrating the masking effect of sedimentation on the spreading features: clear lineations are visible in the Central Atlantic (Figure 2b), but lineations are only poorly distinguishable in the Cape Basin (Figure 2c). In this case, the VGG does little to enhance the spreading lineations (Figure 2d). Derivatives of the gravity anomaly perpendicular to the spreading direction for the Cape Basin were taken after filtering to retain different wavelengths (Figures 2e–2g) to check which wavelengths best enhance spreading features. Shorter wavelengths (25–55 km, Figure 2e) are noisy and reduce the continuity of spreading-parallel anomalies, while longer wavelengths (85–115 km, Figure 2g) reduce the sharpness of individual lineations and can also merge anomalies into false lineations (example indicated by black arrows). Intermediate wavelengths of 55–85 km give the best balance between noise reduction and imaging of sharp FZ-related anomalies.

2.2. Magnetism

We used two primary magnetic data types to inform our final model: the Earth Magnetic Anomaly Grid (EMAG2) [*Maus et al.*, 2009], and published ocean magnetic anomaly interpretations from ship-track data. EMAG2 (nondirectionally gridded version) shows the large-scale trend of magnetic anomalies in the WSB, where many individual linear ocean magnetic anomalies are identifiable. The requirement for orthogonality between these linear ocean magnetic anomalies and identified FZs allowed us to check our interpretation.

Of the published ocean magnetic anomaly interpretations, those by *Ségoufin and Patriat* [1980], *Cochran* [1988], and *Davis et al.* [2016] show strong similarities to each other, with the basin's center of symmetry lying around M0 and the oldest anomalies detected in the basin reaching between M21 and M24. *Rabinowitz et al.* [1983] and *Eagles and König* [2008] choose an alternative interpretation with the basin's center of symmetry around M10 and located significantly farther south. We compare these lines of symmetry with MOR segments identified in the gravity data and used the best matching interpretations to temporally constrain our reconstruction. All interpretations suggest slow-intermediate spreading rates for the WSB.

2.3. Seismic Reflection Data

The East AfricaSPAN seismic reflection lines were used to identify the nature of the top basement reflector and measure the crustal thickness, thus helping determine whether the underlying basement is continental, oceanic, or transitional in nature. In addition, faults associated with the tectonic fabric at mature slow to intermediate spreading centers dip toward the MOR [e.g., *Carbotte and Macdonald*, 1990; *Behn and Ito*, 2008]. Therefore fault polarity switches were used to help constrain the location of the MOR to the east of the DFZ, where spreading ceased ~50 Ma after breakup.

3. Feature Identification

Spreading features of the WSB, including the extinct MOR and FZs, must be detected in order to constrain plate tectonic reconstructions. To do this we identify the characteristics that define each group of features. We must, however, also be careful to avoid interpretation of areas modified by young rifts, such as the Quirimbas Graben, and post-spreading magmatic additions, such as the Comoros Islands, Cosmoledo Group, and Wilkes Rise (e.g., Figure 3), which have strong expressions in the gravity data and mask the true nature of spreading features.

3.1. Mid-Oceanic Ridge Segments

Extinct MOR segments have orientations perpendicular to the final spreading direction, and appear as a free-air gravity low due to a persistent low density gabbroic root [*Jonas et al.*, 1991]. These linear anomalies usually lie close to the basin's center of symmetry, with the exception of basins undergoing subduction, such as the Pacific Ocean [*Müller et al.*, 2008], or those having undergone spreading center reorganization and ridge jumps. To identify the extinct MOR from gravity anomalies, we therefore looked for three characteristics: (1) a linear free-air gravity low, (2) an orientation perpendicular to the approximately N-S

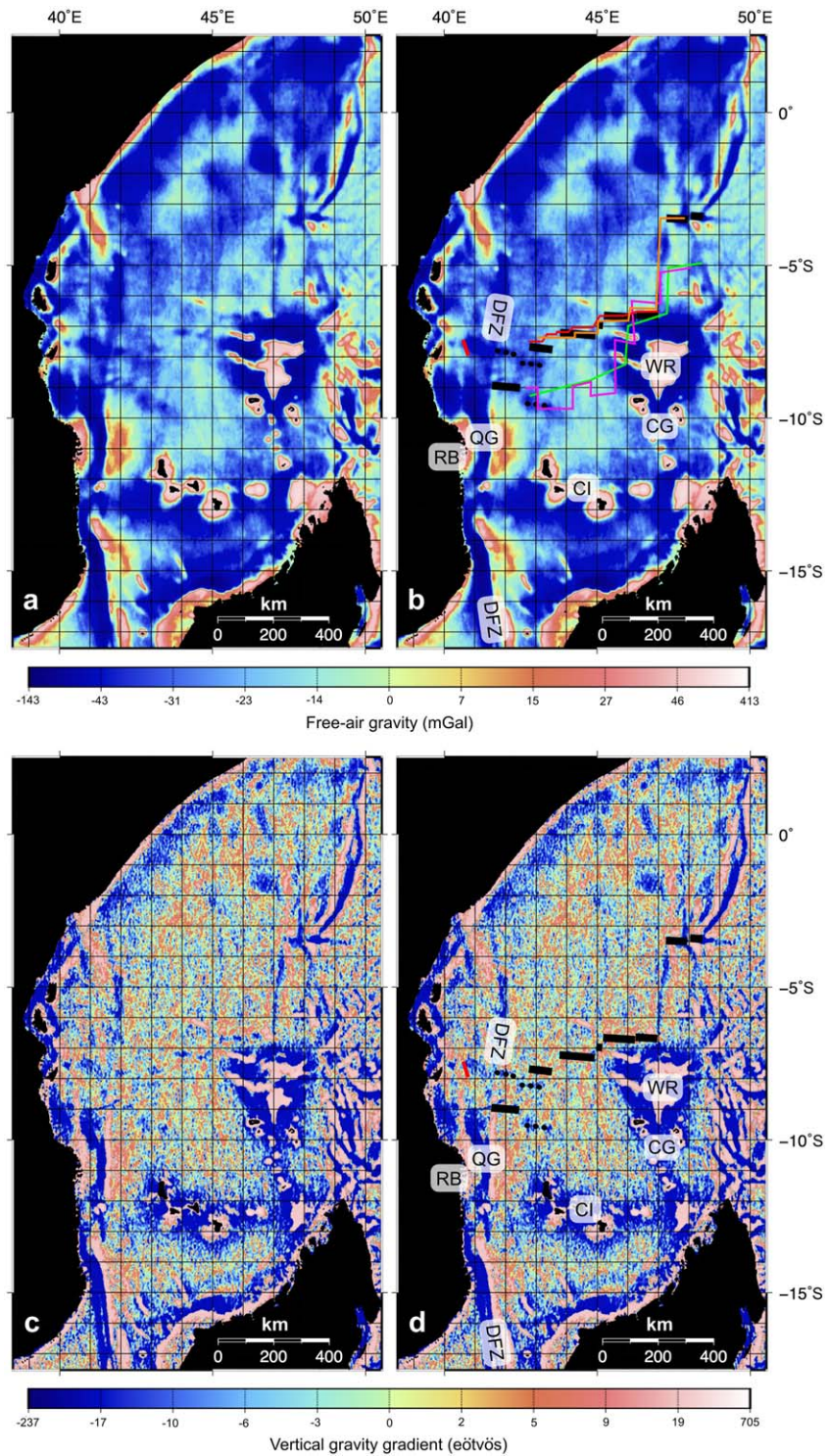


Figure 3. (a) Free-air gravity anomaly. (b) Figure 3a overlain with the picked MOR (solid black lines) and alternative segment possibilities (dashed black lines). Location of the East AfricaSpan seismic reflection line shown in this study is indicated by the thick red line in the Tanzania Coastal Basin. Previously determined basin symmetries are shown as colored lines where constrained by ocean magnetic anomalies. The interpretations of Cochran [1988, orange] and Davis *et al.* [2016, red] are centered on MO and lie in good agreement with the MOR defined by gravity. The interpretations of Coffin and Rabinowitz [1987, green] and Eagles and König [2008, pink] are centered on M10 and deviate significantly from the MOR determined from the gravity data. RB, Rovuma Basin; QG, Quirimbas graben (active rift); DFZ, Davie Fracture Zone. Post-spreading volcanism: CI, Comoros islands; CG, Cosmoledo Group; WR, Wilkes Rise. (c) Vertical gravity gradient. (d) Figure 3c overlain with MOR picks (this study) and abbreviations as for Figure 3b.

paleospreading direction [e.g., *Ségoufin and Patriat*, 1980], and (3) a location close to the axis of symmetry for the WSB. Free-air gravity and VGG maps were used for this task.

Regions where only one gravity lineament with these characteristics was identified provided reliable MOR segment interpretations. These segments were therefore compared with the ocean magnetic anomaly interpretations of *Ségoufin and Patriat* [1980], *Rabinowitz et al.* [1983], *Cochran* [1988], *Eagles and König* [2008], and *Davis et al.* [2016] to assess confidence in these interpretations. Where multiple possible MOR anomalies existed, seismic reflection data were used to locate the MOR using basement fault polarity [e.g., *Behn and Ito*, 2008]. If no seismic data were available, we chose the lineament that was most consistent with the ocean magnetic anomaly interpretations verified by our reliable MOR segments.

3.2. Fracture Zones

In the WSB, 2–5+ km of sediment have accumulated since the Jurassic [*Coffin et al.*, 1986], removing most bathymetric expressions of FZs. A limited set of major lineations related to fracture zones can, however, be seen in the free-air gravity anomaly, reflecting crustal thickness variations, basement offsets, and infilling sediments along the FZs. We further highlighted FZ-related anomalies using a 55–85 km band-pass filter and an E-W directional derivative, orthogonal to the overall N-S spreading direction, as illustrated for the Cape Basin in Figure 2.

The resulting linear anomalies relating to the FZ trends are generally of low amplitude compared with those arising from volcanic edifices or active rifts. This is primarily the result of the FZs' comparatively small scale, greater depth, and lower density contrast across the structural boundary. However, to map FZs, we were primarily interested in fairly continuous linear anomalies that form a consistent pattern, even if low in amplitude due to the thick sedimentary cover. These lineations (e.g., Figure 2f) can be mapped along minima, maxima, or polarity changes in the gravity gradient; all have the same orientation and thus lead to the same plate tectonic model. However, for consistency, we have manually picked along the polarity change in the gravity gradient, except in cases where this is poorly defined and the maximum or minimum shows the orientation more clearly.

The Tanzania Coastal Basin, inboard of the DFZ, has previously been assumed to be underlain by continental crust. To determine whether to interpret any gravity lineations within this basin as continental shear zones or oceanic fracture zones, the East AfricaSPAN seismic reflection data set was used to determine the nature of the crust. Oceanic crust was identified through the recognition of a rough high amplitude top reflector with a tectonic spreading fabric, lacking significant synrift deposits [*Davies et al.*, 2005; *Rodger et al.*, 2006] or by a hummocky reflector with continuous overlying sedimentary deposits [*Soto et al.*, 2011], and, for normal oceanic crust, a two-way travel time (TWTT) between top basement and any Moho reflections of ~ 2 s [e.g., *White et al.*, 1992].

4. Plate Tectonic Reconstruction

After establishing the FZ lineations for the WSB, we used the plate tectonic reconstruction software Gplates [e.g., *Williams et al.*, 2012], populated with the plate polygons of *Seton et al.* [2012], to retrace Madagascar's path back to Africa. The previously identified Dhow and VLCC fracture zones [*Bunce and Molnar*, 1977] were not used as input to the model because *Coffin and Rabinowitz* [1987] suggested they may be the result of tectonic processes other than oceanic spreading. Once the general origin for Madagascar was established, its position was refined by aligning conjugate continental shear zones and sedimentary basins, following *Windley et al.* [1994] and *Reeves* [2014]. Artificial flow lines were then seeded at the deepest points of the basins between Madagascar and Africa according to the CRUST1.0 model [*Laske et al.*, 2013], assumed to be the original center of symmetry for spreading. In an iterative process, the motion of Madagascar away from Africa was then refined by aligning model-generated flow lines with the interpreted fracture zone trends. The plate model was temporally constrained by the ocean magnetic anomaly interpretations of *Cochran* [1988] and *Davis et al.* [2016], whose centers of symmetry around M0 most reliably matched the observed MOR segments. However, no plate velocity constraints exist between the initiation of rifting in the Toarcian (182 Ma) and the oldest ocean magnetic anomaly detected in the basin (M22, 150.5 Ma) [*Cochran*, 1988; *Gradstein et al.*, 2012]. Between the onset of rifting and breakup at 170 Ma in the Bajocian [*Geiger et al.*, 2004], we imposed an extensional velocity of 3.3 mm/yr, similar to the average present day extension rates

along the East African Rift System between Malawi and Afar [Saria *et al.*, 2014]. Following this rifting episode ~ 390 km remained between the spreading center and the M22 magnetic anomaly, which was bridged with a constant velocity of 40 mm/yr.

5. Results

Using free-air gravity, VGG, and directional derivatives of filtered gravity from version 23 of the Sandwell and Smith gravity model, we have detected the extinct MOR segments and a comprehensive set of lineaments relating to spreading features in the Western Somali Basin. These features are tested against magnetic and seismic reflection data before being used to produce a high-resolution plate tectonic reconstruction of the basin.

5.1. MOR Segment Locations

Oceanic magnetic anomalies in the WSB show that spreading occurred in a generally N-S direction [Ségoufin and Patriat, 1980]. Following this, and the NE-SW trends of the Kenya-Somalia and Northern Madagascar coastlines, we expect the extinct MOR to be composed of E-W trending segments with an overall NE-SW trend following the basin's center of symmetry. We identify short linear gravity lows following this pattern in both the free-air gravity anomaly (Figures 3a and 3b) and the VGG (Figures 3c and 3d). The MOR segments generally range from 30 to 100 km in length, with offsets between segments ranging from as little as 20 km up to 350 km between the two easternmost segments.

On the eastern side of the basin, single gravity lineaments point unambiguously to the MOR. This region is therefore used as an independent check of the previous ocean magnetic anomaly interpretations. This shows that interpretations with the basin's center of symmetry based on M0 are most reliable, and therefore the ocean magnetic anomaly interpretations of Cochran [1988] and Davis *et al.* [2016] are used to temporally constrain our plate tectonic model. In the western region of the basin, close to the DFZ, two segments have two or three possible MOR anomalies identifiable in the gravity data (Figure 3, dashed lines). For the westernmost segment, seismic reflection data covers the southern gravity lineament and shows a flip in half graben polarity centered at its location. The next segment to the east is covered by magnetic data along ship tracks and the verified ocean magnetic anomaly interpretations show the northern gravity lineament to be most consistent (Figure 3, solid lines).

5.2. Fracture Zone Trends

The free-air gravity anomaly shows a number of major lineaments in the Western Somali Basin, including the Davie, ARS, Dhow, and VLCC fracture zones, as well as number of more subtle lineaments with a similar trend (Figure 4). Fracture zones in the Indian Ocean, which has much thinner sediment cover (< 1 km) [Whittaker *et al.*, 2013], are also clearly seen. These lineaments often display a significant anomaly in the gravity field, from ~ 20 mGal to over 100 mGal compared to their surroundings, and can be traced for several hundred kilometers, including over 1000 km in the case of the DFZ. They show an arcuate spreading pattern for the Western Somali Basin. This trend can not only be seen in the north of the basin, but is also defined by a striking bend in the DFZ located at 41°E , 14°S , which appears to deflect the trend of the continent-ocean transform margin onshore along the Rovuma Basin.

Lineaments detected only in the filtered and directionally differentiated gravity data are generally shorter and less continuous, ranging in length from less than 100 km up to approximately 600 km (Figure 5). In several instances, extensions to fracture zones detected in the free-air anomaly can be made, such as at 45°E 7°S , where a conjugate fracture zone to one detected in the north becomes apparent in the southern half of the basin. On the whole, these lineaments align with the framework laid out by anomalies detected in the free-air gravity and provide a comprehensive record of plate spreading directions. A few short lineaments, however, lie at significant angles to the general fabric. It is likely that these lineaments are the result of structures unrelated to spreading (which should produce a consistent and predictable network of FZs), such as small volcanic chains or large infilled submarine channels, producing gravity anomalies with a similar wavelength to those of spreading features.

The EMAG2 gridded magnetic data set (Figure 6a) contains several linear magnetic trends within the central region of the WSB, where the basement is oceanic in nature [Coffin *et al.*, 1986]. Away from magmatic structures such as the Wilkes Rise and Comoros Islands, these anomalies should be due to magnetization of

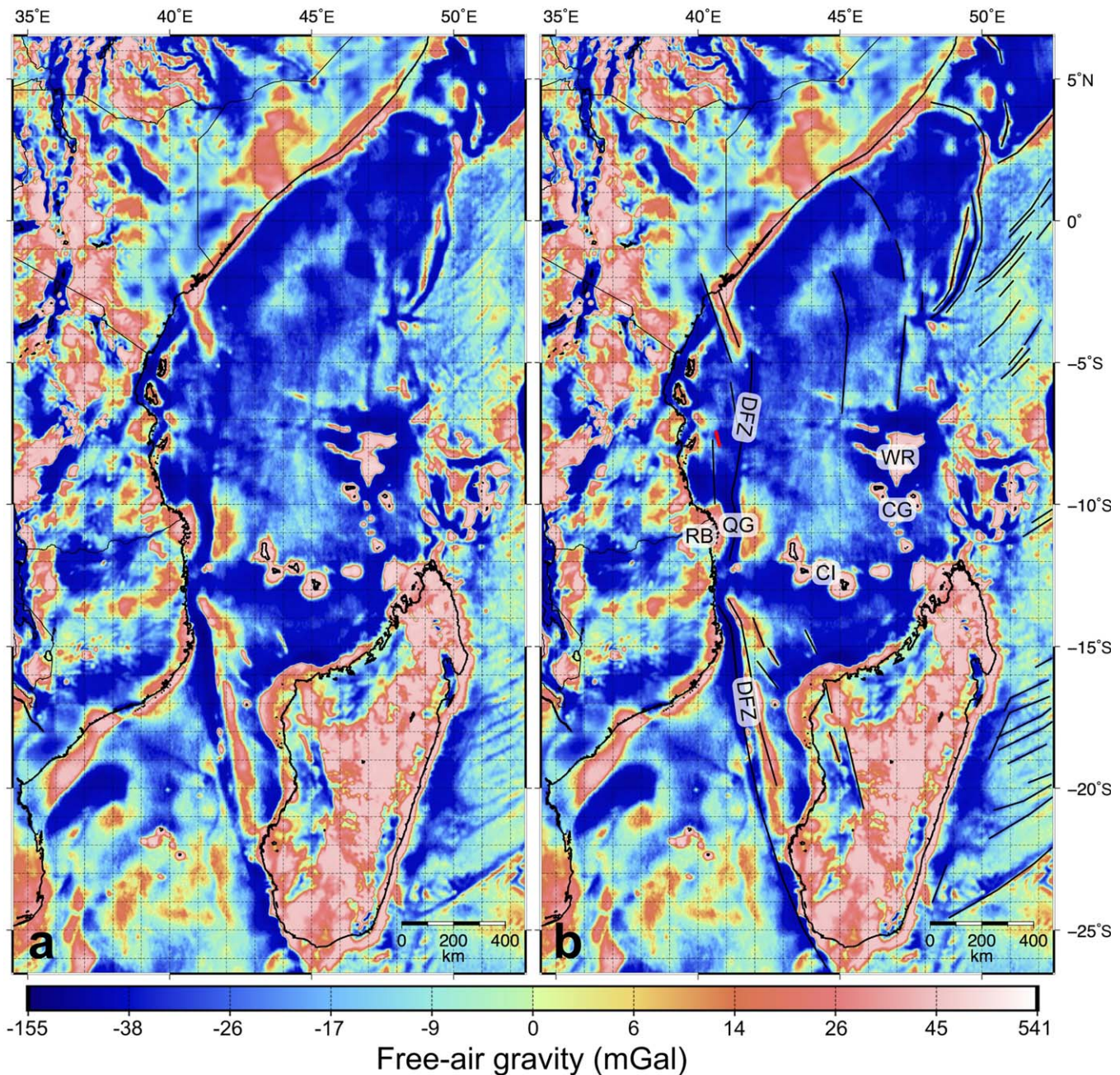


Figure 4. (a) Free-air gravity anomaly. (b) Figure 4a overlain with the linear anomalies related to potential fracture zones. Abbreviations as for Figure 3. Location of the East AfricaSpan seismic reflection line shown in this study is indicated by the red line in the Tanzania Coastal Basin.

oceanic crust during seafloor spreading, producing ocean magnetic anomalies. Their orientation appears variable, and they do not seem to define a consistent spreading direction. When, however, the magnetics are overlain by the FZ trends identified in the gravity data, the linear magnetic anomalies can be seen to lie consistently perpendicular to the arcuate fracture zone lineaments (Figure 6b), providing independent confirmation of our proposed fracture zone structure.

5.3. Plate Tectonic Model

Using our new fracture zone lineaments, shear zone data from *Reeves and De Wit* [2000], and basin depth data from CRUST1.0, we developed a new plate tectonic reconstruction for Madagascar's separation from Africa (Figure 7).

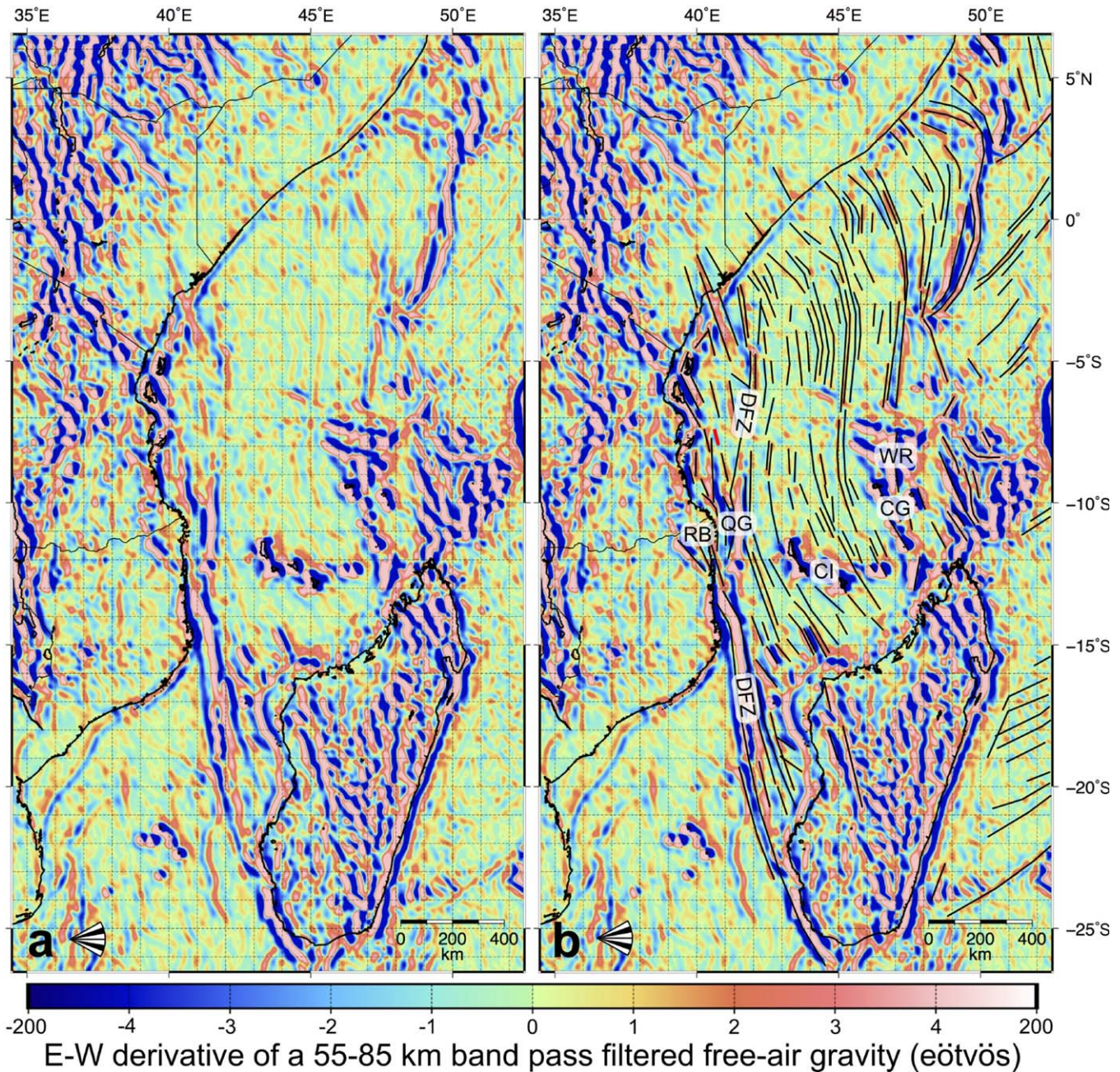


Figure 5. (a) E-W derivative of a Gaussian band-pass filtered free-air anomaly, 50% long and short wavelength cutoffs at 85 and 55 km, respectively, to best retain anomalies related to fracture zones. (b) Figure 5a overlain with the linear anomalies identified here and in Figure 4. Abbreviations as for Figure 3. Location of the East AfricaSpan seismic reflection line shown in this study is indicated by the red line in the Tanzania Coastal Basin.

An initial phase of continental rifting from 182 Ma leads to continental break up at approximately 170 Ma (Figures 7b and 7c). Oceanic spreading commences in a NNW-SSE direction and results in strike-slip tectonics between Madagascar and northern Mozambique, forming the Rovuma Basin (Figure 7c and 7d). At ~150.5 Ma, the spreading direction changes to almost N-S, resulting in the near alignment of several flow lines in the west of the basin (Figure 7d and 7e). After 136 Ma, the spreading direction continues to rotate, causing full convergence of the flow lines in the west of the basin along the trace of the DFZ. Faster spreading in the west compared to the east also results in an anti-clockwise rotation of Madagascar to its present-day position, which was reached when oceanic spreading ceased in the basin at ~125 Ma (Figure 7e and 7f).

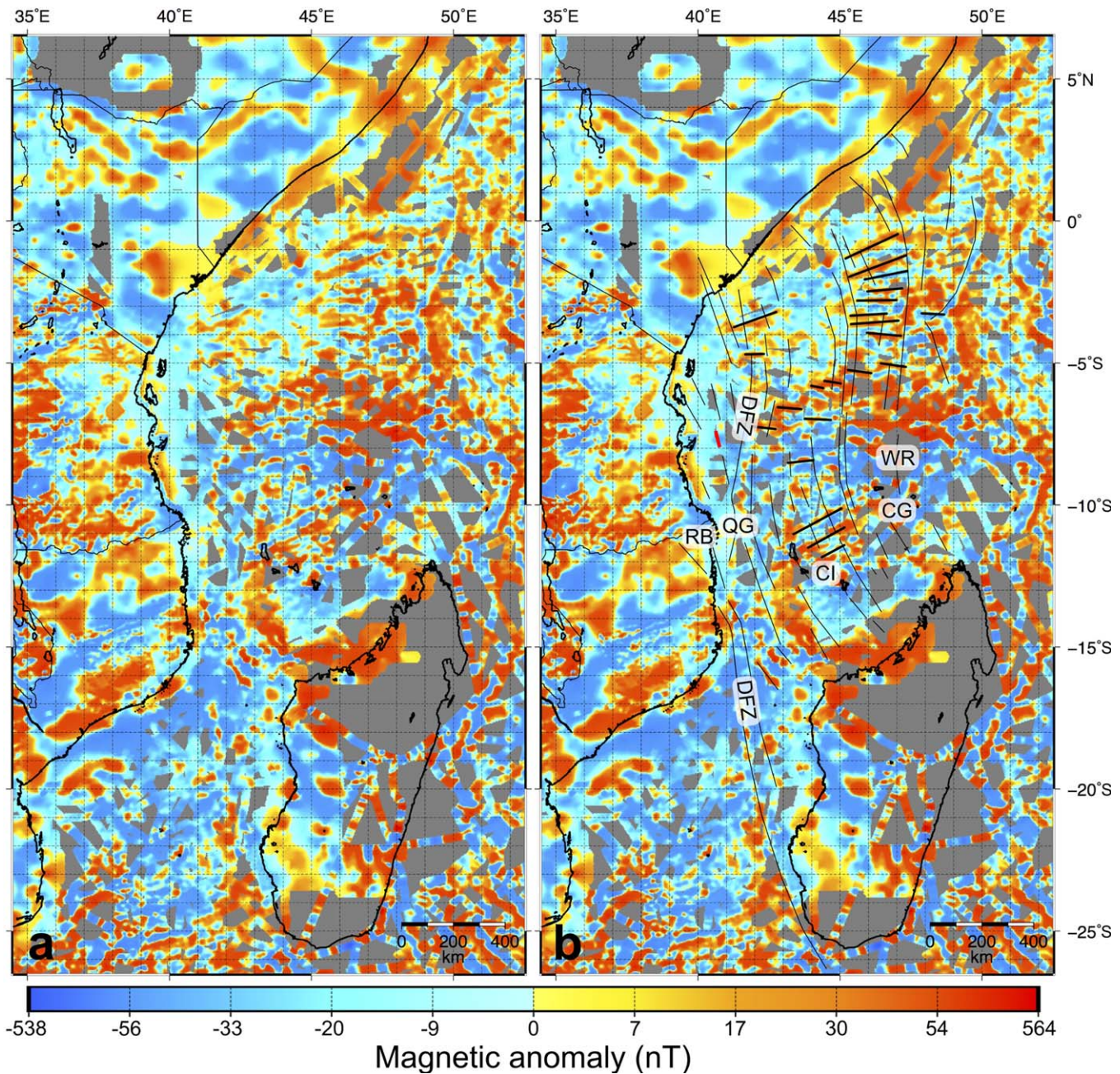


Figure 6. (a) The EMAG2 nondirectionally gridded magnetic anomaly data set. (b) Figure 6a with broadly E-W linear magnetic anomalies detected from unmodified oceanic crust (thick black lines) and fracture zones (thin black lines) marked, showing a consistently orthogonal relationship. Abbreviations as for Figure 3. Location of the East AfricaSpan seismic reflection line shown in this study is indicated by the red line in the Tanzania Coastal Basin.

6. Discussion

6.1. The Nature of the WSB's Margins and of Gravity Lineaments in the Coastal Basins

Modern concepts of passive margin formation define two end-member types. (1) At volcanic rifted margins, crustal thinning occurs over relatively short distances (50–100 km) [e.g., Franke, 2013] and is accompanied by large volumes of magmatism. These are characterized by both thick wedges of volcanic flows that appear as seaward-dipping reflectors in seismic reflection data [e.g., Planke and Eldholm, 1994; Geoffroy, 2005] and by high velocity underplating and heavily intruded crust identified in seismic refraction studies [e.g., Korenaga et al., 2000; Hirsch et al., 2009]. (2) At magma-poor rifted margins, the largely unthinned continental crust of the proximal domain passes into a hyperextended domain containing three sub domains

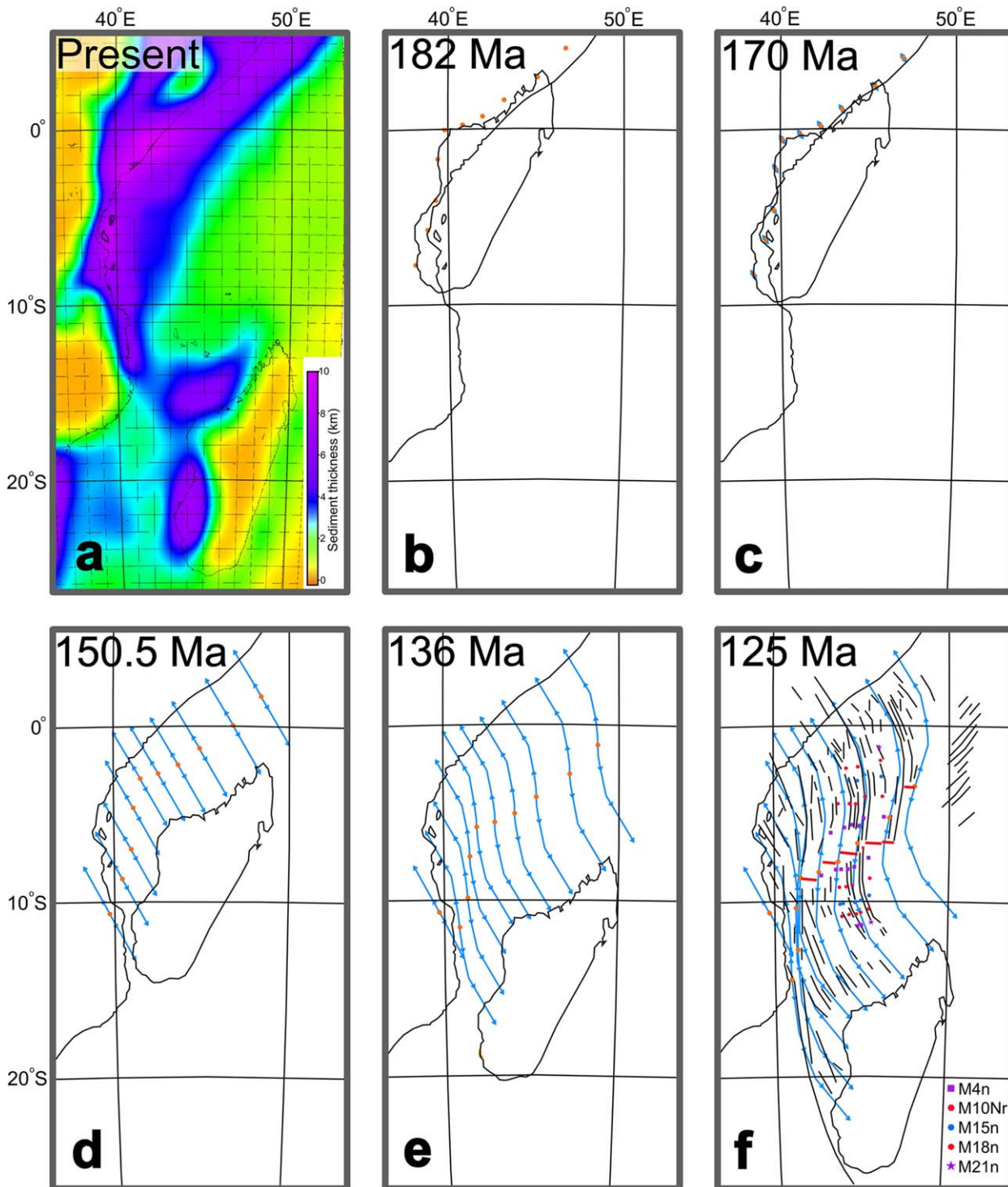


Figure 7. Plate tectonic reconstruction of Madagascar’s escape from Africa from the Early Jurassic to the cessation of spreading in the Cretaceous. Madagascar is shown without the remainder of East Gondwana (India, Antarctica, and Australia) attached. (a) Present-day sediment thickness in the Western Somali Basin taken from the CRUST1.0 model. (b–e) The key stages of Madagascar’s motion out of Africa. Modeled flow lines are shown as blue-arrowed lines where the center of symmetry is marked by orange circles. (f) Madagascar’s present-day position, which is reached at around 125 Ma. Flow lines closely match the fracture zone pattern of the basin (additional black lines), and the basin’s predicted final symmetry (orange circles) lies in good agreement with the interpreted extinct mid-ocean ridge system (red lines). Locations of magnetic anomalies used to temporally constrain plate motions shown with symbols as interpreted by Davis et al. [2016].

(the necking, hyperthinned, and exhumed mantle domains), before oceanic crust marks the onset of the oceanic domain [Tugend et al., 2015]. The necking and hyperthinned domains accommodate most of the crustal thinning, containing continental crust <10 km thick, and typically extend 100–200 km from the

proximal domain [e.g., Reston, 2009; Sutra and Manatschal, 2012]. The exhumed mantle domain forms the continent-ocean transition and is thought to consist of mantle material unroofed and serpentinized during extensional detachment faulting [e.g., Bayrakci et al., 2016; Gillard et al., 2016], which separates continental crust from oceanic crust. These margins characteristically experience limited magmatism during extension [Franke, 2013].

To understand the style of margin formation in the WSB, we draw together a combination of seismic, gravity, magnetic, and geological evidence. Coffin et al. [1986] confirmed the existence of oceanic crust just offshore of the Kenya-Somalia border as far north and west as 42.05°E 2.52°S, but inboard of this within the Tanzania Coastal Basin and extending onshore within the Lamu Embayment, thin crust (<13 km thick) [Reeves et al., 1987] of an ambiguous nature is covered by thick sediments (up to +12 km, Yuan et al. [2012] and references therein). Based on gravity and magnetic modeling, Reeves et al. [1987] proposed that this crust is oceanic in nature, consistent with observations of necking zones (as defined by Tugend et al. [2015]) onshore along the western edge of the Lamu Embayment from seismic refraction data, which suggest sharp crustal thinning from over 40 km to probably less than 15 km at this location [Prodehl et al., 1997]. This implies that offshore seismic reflection data along the Tanzanian and Kenyan margins is located seaward of the necking zones. Ascertaining the margin nature is thus more difficult, since seaward-dipping reflectors, which are characteristic of volcanic margins, form in close proximity to the necking zone and therefore may not be detected, whilst exhumed mantle domains, as seen at magma-poor margins, can be difficult to distinguish from oceanic crust formed at slow spreading centers when using seismic reflection data alone [e.g., Davy et al., 2016].

Furthermore, the already thin crust onshore within the Lamu Embayment suggests that the “shelf edge” high, seen in the free-air gravity along the Somali coast east of the DFZ, is not indicative of crustal thinning, and may not coincide with the continent-ocean transition as proposed elsewhere [e.g., Bauer et al., 2000]. The effects of increasing water depth and thick sedimentary accumulations can also produce this pattern of gravity anomalies without an additional contribution from decreasing crustal thickness [e.g., Walcott, 1972; Watts and Stewart, 1998]. Elsewhere along the western margins of the WSB, no shelf edge gravity anomalies are present, possibly due to superimposed effects of active rifting in the area, providing little information as to the margin nature. However, as there is little evidence for Jurassic rift-related volcanic rocks exposed at the surface in Madagascar, Tanzania, or Kenya [e.g., Guiraud et al., 2005], and neither have they been drilled onshore or offshore (despite the pervasive record of postrift volcanics emplaced in the upper Cretaceous [Coffin and Rabinowitz, 1988] related to the breakup between Madagascar and India [e.g., Storey et al., 1995]), significant magmatism during rifting in the WSB seems unlikely. This apparent lack of rift-related volcanism, the generally thin nature of the oceanic crust interpreted elsewhere within the WSB (5.22 ± 0.64 km) [Coffin et al., 1986], and the lack of any high velocity underplating interpreted around the necking zone from seismic refraction studies [Prodehl et al., 1997] make present observations from the margins of the WSB more consistent with the magma-poor end-member style of rifted margins.

The ambiguous crust within the Tanzania Coastal Basin and Lamu Embayment could therefore be either oceanic, formed after breakup, or hyperextended continental crust and mantle. Whilst the present-day high heat flow along the East African margin (attested by the significant gas discoveries in the region) possibly favors the presence of radiogenic continental crust [e.g., White et al., 2003], active lithospheric thinning along the offshore branch of the East African Rift System [e.g., Delvaux and Barth, 2010; Franke et al., 2015] would also act to increase regional heat flow. In the mid-Tanzania Coastal Basin, inboard of the DFZ, the East AfricaSPAN seismic reflection lines image a strong and continuous reflector at approximately 9.5 s TWTT, which is 1.5–2.3 s TWTT below the top basement (Figure 8). This is typical of slightly thin to normal oceanic crust [White et al., 1992], and is similar to the 1.17–2 s TWTT derived for oceanic crust elsewhere within the WSB [Coffin et al., 1986]. Several areas within the crust are also characterized by low reflectivity, a common property of oceanic crust [e.g., Bécel et al., 2015].

The nature of the crust changes from NNW to SSE along the line. In the NNW, a smooth top basement reflector is imaged at 7.4 s TWTT, which is characteristic of oceanic crust formed by relatively robust magmatic accretion with little tectonic extension [e.g., Reston et al., 2004]. Here an additional reflector can be seen at ~8.3 s TWTT (0.9 s below top basement) which delineates an upper and lower crustal layer. Elsewhere within the WSB, the oceanic layer 2 thickness has been derived as 0.93 s TWTT [Coffin et al., 1986],

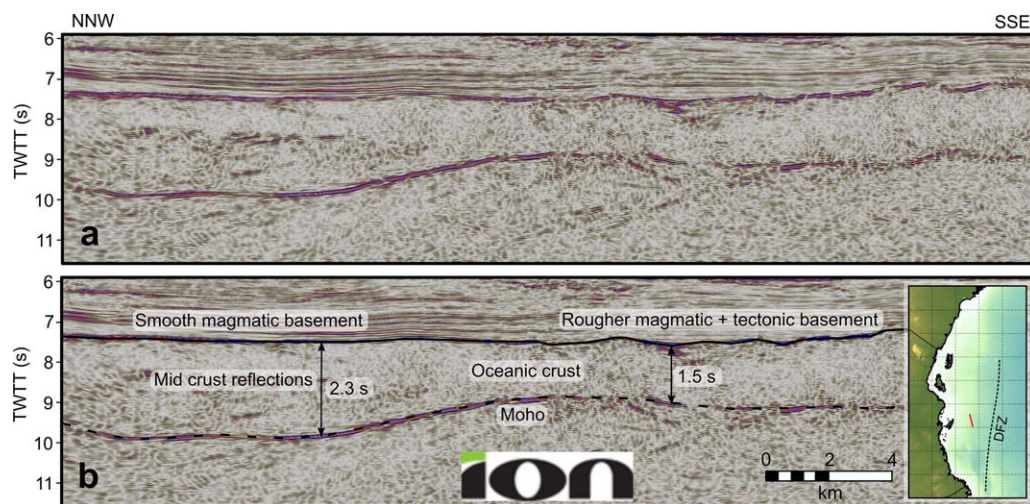


Figure 8. (a) Seismic reflection line from East AfricaSPAN (Ion Geophysical), inboard of the DFZ. (b) Figure 6a with interpretation overlain. Inset shows location relative to the coastline and the DFZ.

and so this reflector may represent the boundary between oceanic layers 2 and 3. The smooth top basement and Moho reflectors also extend ENE along the seismic cross line, perpendicular to the spreading direction, with a consistent offset of between 1.8 and 2 s TWTT, before eventually reaching the tectonically overprinted DFZ, where their character is lost. To the SSE in Figure 8, following a reduction in thickness of the crust demonstrated by the shallowing of the Moho reflector, the top basement gains a weak tectonic fabric. These observations are consistent with a reduction in magma supply and resulting increase in the tectonic extensional component of oceanic spreading [e.g., Reston *et al.*, 2004].

Alternatively, the Moho reflector could represent a detachment fault formed between continental crust and mantle during hyperextension [e.g., Tugend *et al.*, 2015], such as the S reflector west of Galicia [Hoffmann and Reston, 1992] and H reflector in the Iberia Abyssal Plain [Dean *et al.*, 2008]. However, the smooth top basement reflector lacks the well-defined fault blocks often imaged in such hyperextended domains [Reston, 2009]. This suggests that extreme crustal extension is unlikely, especially as rift-related volcanism, which could otherwise have masked fault block topography, is extremely limited during hyperextension at magma-poor margins [Franke, 2013].

All these observations thus support high levels of extension, probably including oceanic crust, in the mid-Tanzania Coastal Basin inboard of the DFZ. The DFZ cannot then be a simple continent-ocean transform margin. Instead, Madagascar must have originated from within the Tanzania Coastal Basin and Lamu Embayment, with the Rovuma Basin forming the continent-ocean transform margin. The onshore trend of this basin is closely aligned with the early SSE trending fracture zones detected in the gravity data (Figure 9b), and in fact, in our plate tectonic reconstructions, strike-slip motion of southern Madagascar along this basin is unavoidable. This is in good agreement with observations of dextral strike-slip faults along the Rovuma Basin margin [Emmel *et al.*, 2011] and an onshore sedimentary thickness of ~ 10 km in the northern Rovuma Basin that rapidly thins westward to < 1 km [Key *et al.*, 2008], consistent with a continent-ocean transform margin. As noted by Reeves [2014], the passage of Madagascar along the Rovuma Basin also allows for a much tighter and more consistent fit of Gondwana fragments, reducing the need for gaps and unsmooth plate motions during Gondwana's disassembly.

6.2. Rifting Mechanisms and Gondwana Breakup

Rifting between East and West Gondwana began in the Toarcian [Geiger *et al.*, 2004] and was probably initiated by the eruption of the Bouvet plume, resulting in a contemporaneous volcanic passive margin in Mozambique [Klausen, 2009]. Here, an 8.5 km thick suite of rift-related basalts and rhyodacites defines a relatively narrow volcanic margin, where a magmatic mode of extension dominated in the lead-up to breakup [Klausen, 2009]. This section of the rift system developed discordantly to the structural trend of Gondwana's

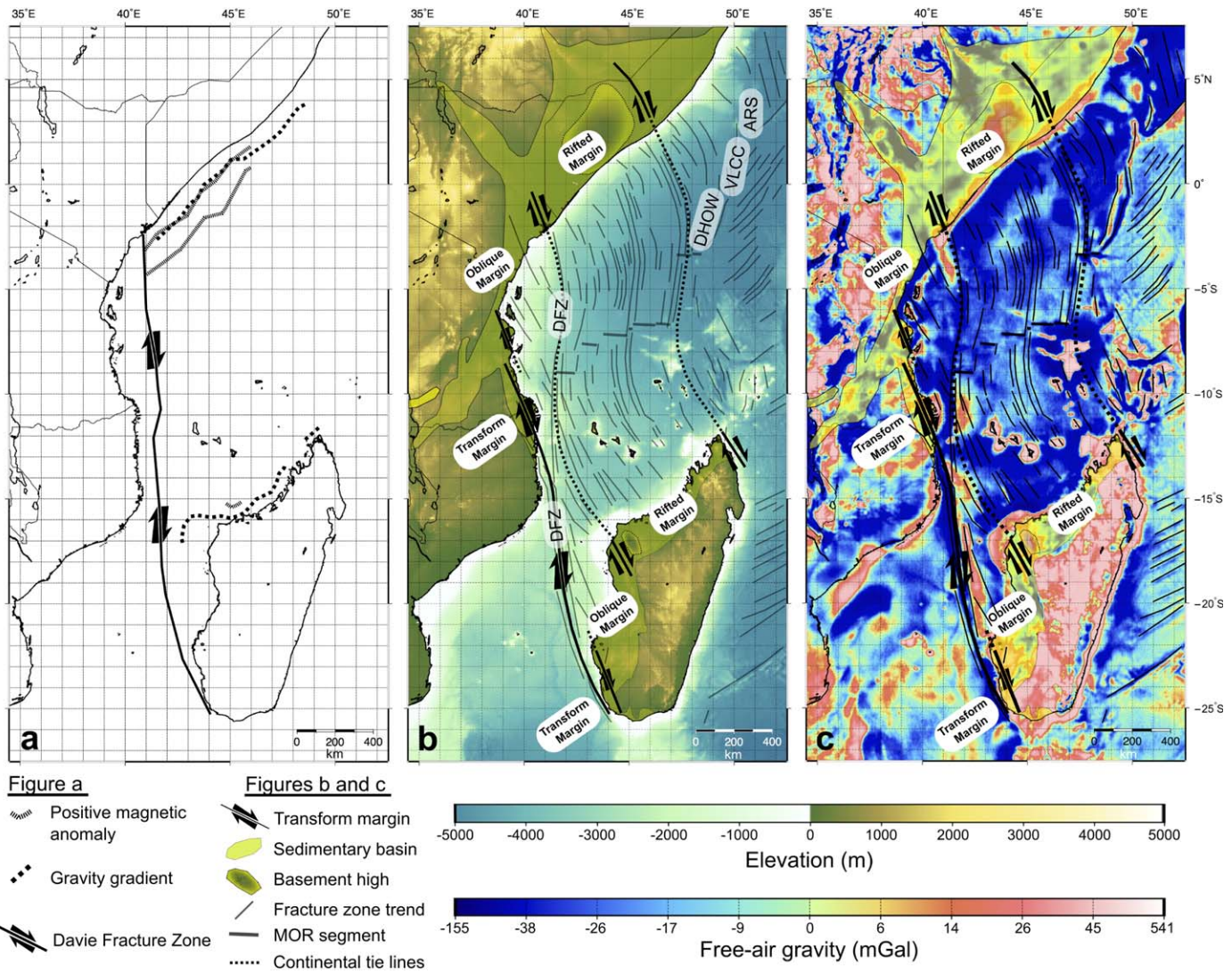


Figure 9. (a) Commonly interpreted basin configuration, where the continent-ocean transition is assumed to follow the DFZ [e.g., Bunce and Molnar, 1977; Coffin and Rabinowitz, 1987; Gaina et al., 2013]. (b) Schematic of the basin configuration suggested in this study, with strike-slip tectonics dominating along the edge of the Rovuma Basin, while much of the Tanzania Coastal Basin should be considered as an obliquely rifted margin. The Davie Fracture Zone is a major ocean-ocean fracture zone, not the continent-ocean transform margin. DFZ, Davie Fracture Zone; DHOW, Dhow Fracture Zone; VLCC, Very Large Crude Carrier Fracture Zone; ARS, Auxiliary Rescue and Salvage Fracture Zone. (c) Free-air gravity overlain with interpretation as for Figure 9b.

sedimentary basins [Salman and Abdula, 1995], suggesting that preexisting lithospheric structure was not a key parameter leading to breakup.

In the Western Somali Basin, however, there is little evidence for a magmatic breakup, as discussed earlier (section 6.1). This is most likely a function of the WSB's distance from the volcanic center in Mozambique as seen in the Gulf of Aden. Here, volcanic margins formed close to the Afar hotspot, yet farther away, east of longitude 46°E, the margins are magma-poor [Leroy et al., 2012]. Breakup along the Tanzanian-Kenyan and Kenyan-Somalian rift sections is therefore less likely to have been influenced by magmatism and thermal weakening of the lithosphere [Buck, 2007]. It is apparent from the spreading lineaments detected in the WSB that initial spreading occurred in a NNW-SSE direction, in agreement with principal extensional stresses around the Mozambique basin [Le Gall et al., 2005]. This is consistent with the occurrence of strike-slip tectonics along the NNW-SSE trending Rovuma Basin and oblique rifting along the N-S trending Kenya-Tanzania margin (Figure 9b), both of which are mechanically favorable [Emmel et al., 2011; Brune et al., 2012]. This is similar to observations from the Gulf of California where oblique rifting assisted continental breakup through the efficient focusing of crustal thinning within pull-apart basins bounded by large offset

strike-slip faults [Bennett and Oskin, 2014]. If this mechanism was active during the Jurassic rifting along the Tanzania-Kenya margins, it may explain the possible margin segmentation suggested by the stepped shape of Madagascar's western coastline. Margin segmentation is common to many oblique passive margins worldwide [e.g., Leroy *et al.*, 2012; Bennett and Oskin, 2014].

Conversely, the NE-SW trending Kenyan-Somalian rifted margin formed orthogonally to the breakup direction. Although the Rovuma basin shows little evidence of Karoo age rifting and sedimentation [Smelror *et al.*, 2008], the Morondava, Majunga, and Ambilobe basins of Madagascar all contain underlying Karoo sediments [e.g., Hankel, 1994]. The conjugate margins on the mainland, the Tanzanian-Kenyan and Kenyan-Somalian rift systems, thus appear to have followed the preexisting lithospheric structure of the Karoo rift system. A transition can therefore be proposed along the East African margin from predominantly strike-slip tectonics and oblique rifting in the Rovuma Basin, progressing northward to oblique rifting that also follows preexisting lithospheric structures along the Tanzanian-Kenyan section, and finally, purely orthogonal rifting along preexisting lithospheric structure in the Kenyan-Somalian section. This is consistent with oblique rifting [Brune *et al.*, 2012] and preexisting lithospheric structure [e.g., Audet and Burgmann, 2011] assisting supercontinent breakup.

The rifting between East and West Gondwana therefore provides a good natural laboratory for the study of the spatially variable interplay between different rifting mechanisms during supercontinent breakup. Examples where each of the proposed facilitating mechanisms (magmatism, oblique rifting, and preexisting structure) appears to dominate during breakup can be seen along the Gondwana rift system between Mozambique and Somalia, with predominantly magmatic breakup in the Mozambique Basin, apparent strike-slip and oblique tectonics along the Rovuma Basin, and coincident preexisting lithospheric structure along the Kenyan-Somalian coast. Analogy can be made to the opening of the South Atlantic during breakup of the supercontinent Pangea, where evidence supports similar regional variation in breakup mechanism. Here, a south to north transition from magmatically dominated breakup in the southern South Atlantic [e.g., Gibson *et al.*, 2006], inheritance-driven rifting in the central South Atlantic [e.g., Lentini *et al.*, 2010], and strongly oblique rifting in the Equatorial Atlantic [Heine and Brune, 2014] is seen. Together, these margins suggest that rifting during supercontinent dispersal may often be facilitated by multiple mechanisms, with regional variation along the margin due to different preexisting geological structures and changing tectonic geometry on length scales as short as a few hundred kilometers.

6.3. Plate Tectonic Reconstruction

For the initial rifting phase, we impose a plate separation rate of 3.3 mm/yr, similar to that of the present-day East African Rift System between Malawi and Afar [Saria *et al.*, 2014]. Breakup occurred at approximately 170 Ma, as evidenced by the Early Bajocian breakup unconformity identified in the Morondava Basin [Geiger *et al.*, 2004] and the overwhelming transition to marine deposits along the East Africa margins at this time [Coffin and Rabinowitz, 1992]. Between breakup and the earliest magnetic anomaly constraint (M22), an average full spreading rate of 40 mm/yr therefore occurred, similar to the average full spreading rate of ~ 49 mm/yr determined by ocean magnetic anomalies for the younger oceanic crust between M22 and M0 [Cochran, 1988; Davis *et al.*, 2016].

Following this initial phase of spreading, which resulted in strike-slip motion between Madagascar and the Rovuma Basin, a rotation in the spreading direction occurred at ~ 150.5 Ma. The oldest conjugate pair of magnetic anomalies detected, M22 [Cochran, 1988; Davis *et al.*, 2016], constrains the age of this rotation, which is contemporaneous with Madagascar's exit from the SSE trending Rovuma Basin, after which it began to follow a N-S spreading direction. This rotation began the cessation of any oceanic spreading in the Tanzania Coastal Basin and offshore Morondava Basin as flow lines began to align along what was to become the DFZ (Figures 7d and 7e). This alignment suggests strike-slip tectonics began to dominate along this zone, and it is therefore possible that the DFZ formed at this point as several fracture zones coalesced into one major oceanic fracture zone with a significant accumulated offset.

Following the first rotation in plate motions at 150.5 Ma, spreading continued relatively undisturbed in the Western Somali Basin until approximately 136 Ma, when a further change in plate motion occurred contemporaneous with Madagascar's departure from the Mozambique continental transform margin. This rotation further aligned the flow lines along the DFZ as it became the dominant strike-slip fault in the basin. From

here until the termination of oceanic spreading at M0 (125 Ma), Madagascar underwent a gentle anti-clockwise rotation to take its present-day position relative to Africa.

The termination points for our model flow lines lie very close to the extinct MOR identified in the gravity data. We emphasize that this striking agreement is generated only from our fracture zone trends and initial seed points for the flow lines, which were chosen independently based on the CRUST1.0 data set, and thus provides strong confirmation of the model. No ocean magnetic anomalies have been identified to help constrain the location of the westernmost segment of the MOR. However, seismic reflection data suggests a southerly location for the MOR segment, in line with the symmetry predicted from the plate tectonic reconstruction.

A key result of the reconstruction is that the DFZ is shown to be a major ocean-ocean FZ, where oceanic crust has formed inboard of this feature within the Tanzania Coastal Basin. This challenges many plate tectonic reconstructions which, based on the previously available literature, have defined the DFZ as the continent-ocean transform margin of the Western Somali Basin [e.g., *Gaina et al.*, 2013], an important constraint on spreading kinematics. As the DFZ is a predominantly straight feature, treating it as the continent-ocean transition naturally results in the prediction of a less complex spreading pattern (i.e., only ~N-S without an initial NNW-SSE component) and a looser fit of Gondwana fragments due to the inability to reconstruct continents inboard of the DFZ. However, by detailed analysis of spreading lineaments on a small scale, we have been able to resolve the initial NNE-SSW spreading stage. This is in agreement with NNW-SSE principal extensional stresses during breakup around the Mozambique basin, recorded from dyke dilation in the Okavango and Limpopo dyke swarms [*Le Gall et al.*, 2005]. This spreading pattern is also strikingly similar to spreading patterns extrapolated to the WSB basin from the Mozambique basin, where they were derived from magnetic anomalies and FZs [*Eagles and König*, 2008]. This suggests that during the earlier stages of spreading, Madagascar and Antarctica shared a similar breakup history, and moved as a cohesive unit away from Africa, as opposed to an amalgamation of continental blocks with relative motions between them. This highlights the importance of basin scale reconstructions in deciphering supercontinent dispersal mechanisms, as well as their potential for constraining the histories of neighboring basins that lack detailed kinematic indicators and for informing larger regional reconstructions.

The Dhow and VLCC fracture zones as interpreted by *Bunce and Molnar* [1977] were not used as input to the plate tectonic model since they may have formed by processes other than oceanic spreading [*Coffin and Rabinowitz*, 1987]. However, their trends are independently predicted by our plate model, so they are likely to have been originally formed as the result of plate spreading after all. Reactivation of these structures may have occurred during the breakup of Madagascar and India, resulting in their more prominent expression in the gravity data compared to other fracture zones in the WSB.

7. Conclusions

Using new techniques to analyze the latest Sandwell and Smith gravity data sets (V23), we have detected the location of the extinct MOR segments and, for the first time, a comprehensive set of fracture zone lineaments within the Western Somali Basin. We have used these to constrain Madagascar's position in Africa prior to breakup, validate ocean magnetic anomaly interpretations for the WSB, and construct a well constrained, high-resolution plate tectonic reconstruction for the region. This plate tectonic reconstruction bears strong similarities to reconstructions from the neighboring Mozambique Basin, and may suggest that East Gondwana broke off from West Gondwana as a cohesive unit, rather than as an amalgamation of continental blocks with relative motions between them. During this disassembly, no single parameter leads to breakup along the entire margin, with thermal weakening due to magmatism, oblique rifting, and preexisting structure apparently dominating in turn from south to north along the Jurassic Gondwana rifts.

The discovery of oceanic crust in the Tanzania Coastal Basin, fracture zone orthogonality to regional magnetic anomalies, and observations from the Rovuma Basin support this reconstruction, and show that the Davie Fracture Zone is a major ocean-ocean fracture zone, formed by the coalescence of several smaller fracture zones during changing spreading directions, and not a continent-ocean transform margin. The western edge of the basin is thus defined by a transform margin in the Rovuma Basin, whereas the Tanzanian and Kenyan margins formed in an oblique regime and are most likely segmented, magma-poor rifted margins. The change in the location and nature of the continent ocean transition has important implications

for the nature of the lithosphere underlying the western portion of the basin, and thus for its thermal history and resource potential.

Acknowledgments

This research is funded by ENI (contract 3500027704), and their financial and data support is greatly appreciated. We thank ION Geophysical for kindly allowing the use of the East AfricaSPAN seismic reflection data set within this research. We would also like to thank Cindy Ebinger and an anonymous reviewer whose constructive comments significantly improved this manuscript. The gravity data used in this study were obtained freely from the Scripps Institution of Oceanography (http://topex.ucsd.edu/www_html/mar_grav.html).

References

- Arrowsmith, J. R., and O. Zielke (2009), Tectonic geomorphology of the San Andreas Fault zone from high resolution topography: An example from the Cholame segment, *Geomorphology*, *113*, 70–81.
- Audet, P., and R. Burgmann (2011), Dominant role of tectonic inheritance in supercontinent cycles, *Nat. Geosci.*, *4*, 184–187.
- Bauer, K., S. Neben, B. Schreckenberger, R. Emmermann, K. Hinz, N. Fechner, K. Gohl, A. Schulze, R. B. Trumbull, and K. Weber (2000), Deep structure of the Namibia continental margin as derived from integrated geophysical studies, *J. Geophys. Res.*, *105*, 25,829–25,853, doi:10.1029/2000JB900227.
- Bayraktir, G., et al. (2016), Fault-controlled hydration of the upper mantle during continental rifting, *Nat. Geosci.*, *9*, 384–388.
- Bécel, A., D. J. Shillington, M. R. Nedimović, S. C. Webb, and H. Kuehn (2015), Origin of dipping structures in fast-spreading oceanic lower crust offshore Alaska imaged by multichannel seismic data, *Earth Planet. Sci. Lett.*, *424*, 26–37.
- Beglinger, S. E., M. P. Corver, H. Doust, S. Cloetingh, and A. K. Thurmond (2012), A new approach of relating petroleum system and play development to basin evolution: An application to the conjugate margin Gabon coastal and Almada-Camamu basins, *AAPG Bull.*, *96*, 953–982.
- Behn, M. D., and G. Ito (2008), Magmatic and tectonic extension at mid-ocean ridges: 1. Controls on fault characteristics, *Geochem. Geophys. Geosyst.*, *9*, Q08O10, doi:10.1029/2008GC001965.
- Bennett, S. E. K., and M. E. Oskin (2014), Oblique rifting ruptures continents: Example from the Gulf of California shear zone, *Geology*, *42*, 215–218.
- Blackman, D. K., and D. W. Forsyth (1991), Isostatic compensation of tectonic features of the mid-Atlantic Ridge: 25–27°30'S, *J. Geophys. Res.*, *96*, 11,741–11,758.
- Brune, S., A. A. Popov, and S. V. Sobolev (2012), Modeling suggests that oblique extension facilitates rifting and continental break-up, *J. Geophys. Res.*, *117*, B08402, doi:10.1029/2011JB008860.
- Buck, W. R. (2007), Dynamic processes in extensional and compressional settings: The dynamics of continental breakup and extension, in *Treatise on Geophysics*, edited by Gerald Schubert, pp. 335–376, Elsevier, Amsterdam.
- Bunce, E. T., and P. Molnar (1977), Seismic reflection profiling and basement topography in the Somali basin: Possible fracture zones between Madagascar and Africa, *J. Geophys. Res.*, *82*, 5305–5311.
- Carbotte, S. M., and K. C. Macdonald (1990), Causes of variation in fault-facing direction on the ocean floor, *Geology*, *18*, 749–752, doi:10.1130/0091-7613(1990)018<0749:COVIF>2.3.CO;2.
- Cochran, J. R. (1988), Somali basin, chain ridge, and origin of the Northern Somali Basin gravity and geoid low, *J. Geophys. Res.*, *93*, 11,985–12,008.
- Coffin, M. F., and P. D. Rabinowitz (1992), The Mesozoic East African and Madagascar conjugate continental margins, *Am. Assoc. Pet. Geol. Mem.*, *53*, 207–240.
- Coffin, M. F., P. D. Rabinowitz, and R. E. Houtz (1986), Crustal structure in the Western Somali Basin, *Geophys. J. R. Astron. Soc.*, *86*, 331–369.
- Coffin, M. F., and P. D. Rabinowitz (1987), Reconstruction of Madagascar and Africa: Evidence from the Davie fracture zone and western Somali Basin, *J. Geophys. Res.*, *92*, 9385–9406, doi:10.1029/JB092iB09p09385.
- Coffin, M. F., and P. D. Rabinowitz (1988), *Evolution of the Conjugate East African-Madagascan Margins and the Western Somali Basin*, The Geological Society of America, Special Paper 226.
- Collette, B. J. (1974), Thermal contraction joints in a spreading seafloor as origin of fracture zones, *Nature*, *251*, 299–300.
- Davies, R. J., C. J. MacLeod, R. Morgan, and S. E. Briggs (2005), Termination of a fossil continent-ocean fracture zone imaged with three-dimensional seismic data: The Chain Fracture Zone, eastern equatorial Atlantic, *Geology*, *33*, 641–644.
- Davis, J. K., L. A. Lawver, I. O. Norton, and L. M. Gahagan (2016), New Somali Basin magnetic anomalies and a plate model for the early Indian Ocean, *Gondwana Res.*, *34*, 16–28.
- Dean, S. M., T. A. Minshull, and R. B. Whitmarsh (2008), Seismic constraints on the three-dimensional geometry of low-angle intracrustal reflectors in the Southern Iberia Abyssal Plain, *Geophys. J. Int.*, *175*, 571–586.
- Delvaux, D., and A. Barth (2010), African stress pattern from formal inversion of focal mechanism data, *Tectonophysics*, *482*, 105–128.
- Eagles, G. (2007), New angles on South Atlantic opening, *Geophys. J. Int.*, *168*, 353–361.
- Eagles, G., and M. König (2008), A model of plate kinematics in Gondwana breakup, *Geophys. J. Int.*, *173*, 703–717.
- Emmel, B. R., Kumar, K. Ueda, J. Jacobs, M. C. Daszinnies, R. J. Thomas, and R. Matola (2011), Thermochronological history of an orogenic passive margin system: An example from northern Mozambique, *Tectonics*, *30*, TC2002, doi:10.1029/2010TC002714.
- Franke, D. (2013), Rifting, lithosphere breakup and volcanism: Comparison of magma-poor and volcanic rifted margins, *Mar. Pet. Geol.*, *43*, 63–87.
- Franke, D., W. Jokat, S. Ladage, H. Stollhofen, J. Klimke, R. Lutz, E. S. Mahanjane, A. Ehrhardt, and B. Schreckenberger (2015), The offshore East African Rift System: Structural framework at the toe of a juvenile rift, *Tectonics*, *34*, 2086–2104, doi:10.1002/2015TC003922.
- Geoffroy, L. (2005), Volcanic passive margins, *Comptes Rendus Geoscience*, *337*, 1395–1408. [Available at <http://dx.doi.org/10.1016/j.crte.2005.10.006>].
- Gaina, C., T. H. Torsvik, D. J. J. van Hinsbergen, S. Medvedev, S. C. Werner, and C. Labails (2013), The African Plate: A history of oceanic crust accretion and subduction since the Jurassic, *Tectonophysics*, *604*, 4–25.
- Geiger, M., D. N. Clark, and W. Mette (2004), Reappraisal of the timing of the breakup of Gondwana based on sedimentological and seismic evidence from the Morondava Basin, Madagascar, *J. Afr. Earth Sci.*, *38*, 363–381.
- Gente, P., R. A. Pockalny, C. Durand, C. Deplus, M. Maia, G. Ceuleneer, C. Mével, M. Cannat, and C. Laverne (1995), Characteristics and evolution of the segmentation of the Mid-Atlantic Ridge between 20°N and 24°N during the last 10 million years, *Earth Planet. Sci. Lett.*, *129*, 55–71.
- Gibson, S. A., R. N. Thompson, and J. A. Day (2006), Timescales and mechanisms of plume–lithosphere interactions: 40Ar/39Ar geochronology and geochemistry of alkaline igneous rocks from the Paraná–Etendeka large igneous province, *Earth Planet. Sci. Lett.*, *251*, 1–17.
- Gillard, M., G. Manatschal, and J. Autin (2016), How can asymmetric detachment faults generate symmetric Ocean Continent Transitions, *Terra Nova*, *28*, 27–34.
- Gradstein, F., J. Ogg, M. Schmitz, and G. Ogg (2012), *The Geologic Time Scale 2012*, 1144 pp., Elsevier, Oxford.

- Guiraud, R., W. Bosworth, J. Thierry, and A. Delplanque (2005), Phanerozoic geological evolution of Northern and Central Africa: An overview, *J. Afr. Earth Sci.*, *43*, 83–143.
- Hankel, O. (1994), Early Permian to Middle Jurassic rifting and sedimentation in East Africa and Madagascar, *Geol. Rundsch.*, *83*, 703–710.
- Heine, C., and S. Brune (2014), Oblique rifting of the Equatorial Atlantic: Why there is no Saharan Atlantic Ocean, *Geology*, *42*, 211–214.
- Hirsch, K. K., K. Bauer, and M. Scheck-Wenderoth (2009), Deep structure of the western South African passive margin: Results of a combined approach of seismic, gravity and isostatic investigations, *Tectonophysics*, *470*, 57–70.
- Hoffmann, H.-J., and T. J. Reston (1992), Nature of the S reflector beneath the Galicia Banks rifted margin: Preliminary results from prestack depth migration, *Geology*, *20*, 1091–1094.
- Jonas, J., S. Hall, and J. F. Casey (1991), Gravity anomalies over extinct spreading centers: A test of gravity models of active centers, *J. Geophys. Res.*, *96*, 11,759–11,777.
- Key, R. M., R. A. Smith, M. Smelror, O. M. Sæther, T. Thorsnes, J. H. Powell, F. Njange, and E. B. Zandamela (2008), Revised lithostratigraphy of the Mesozoic-Cenozoic succession of the onshore Rovuma Basin, northern coastal Mozambique, *S. Afr. J. Geol.*, *111*, 89–108.
- Kim, S.-S., and P. Wessel (2011), New global seamount census from altimetry-derived gravity data, *Geophys. J. Int.*, *186*, 615–631.
- Klausen, M. B. (2009), The Lebombo monocline and associated feeder dyke swarm: Diagnostic of a successful and highly volcanic rifted margin?, *Tectonophysics*, *468*, 42–62.
- Korenaga, J., W. S. Holbrook, G. M. Kent, P. B. Kelemen, R. S. Detrick, H. C. Larsen, J. R. Hopper, and T. Dahl-Jensen (2000), Crustal structure of the southeast Greenland margin from joint refraction and reflection seismic tomography, *J. Geophys. Res.*, *105*, 21,591–21,614.
- Laske, G., G. Masters, Z. Ma, and M. E. Pasyanos (2013), Update on CRUST1.0: A 1-degree Global Model of Earth's Crust, Abstract EGU2013-2658 presented at 2013 EGU General Assembly EGU, Vienna, Austria, 7–12 Apr.
- Le Gall, B., G. Tshoso, J. Dymont, A. Basira Kampunzu, F. Jourdan, G. Féraud, H. Bertrand, C. Aubourg, and W. Vétel (2005), The Okavango giant mafic dyke swarm (NE Botswana): Its structural significance within the Karoo Large Igneous Province, *J. Struct. Geol.*, *27*, 2234–2255.
- Lentini, M. R., S. I. Fraser, H. S. Sumner, and R. J. Davies (2010), Geodynamics of the central South Atlantic conjugate margins: Implications for hydrocarbon potential, *Pet. Geosci.*, *16*, 217–229.
- Leroy, S., et al. (2012), From rifting to oceanic spreading in the Gulf of Aden: A synthesis, *Arab. J. Geosci.*, *5*, 859–901.
- Lottes, A. L., and D. B. Rowley (1990), Reconstruction of the Laurasian and Gondwanan segments of Permian Pangaea, *Geol. Soc. London Mem.*, *12*, 383–395.
- Maus, S., et al. (2009), EMAG2: A 2-arc min resolution Earth Magnetic Anomaly Grid compiled from satellite, airborne, and marine magnetic measurements, *Geochem. Geophys. Geosyst.*, *10*, Q08005, doi:10.1029/2009GC002471.
- Menard, H. W., and T. Atwater (1969), Origin of fracture zone topography, *Nature*, *222*, 1037–1040.
- Mitchell, N. C., and Y. Park (2014), Nature of crust in the central Red Sea, *Tectonophysics*, *628*, 123–139.
- Mulder, T. F. A., and B. J. Collette (1984), Gravity anomalies over inactive fracture zones in the central North Atlantic, *Mar. Geophys. Res.*, *6*, 383–394.
- Müller, R. D., M. Sdrolias, C. Gaina, and W. R. Roest (2008), Age, spreading rates, and spreading asymmetry of the world's ocean crust, *Geochem. Geophys. Geosyst.*, *9*, Q04006, doi:10.1029/2007GC001743.
- Nance, D. R., and B. J. Murphy (2013), Origins of the supercontinent cycle, *Geosci. Front.*, *4*, 439–448.
- Planke, S., and O. Eldholm (1994), Seismic response and construction of seaward dipping wedges of flood basalts: Vøring volcanic margin, *J. Geophys. Res.*, *99*, 9263–9278.
- Prodehl, C., J. R. R. Ritter, J. Mechie, G. R. Keller, M. A. Khan, B. Jacob, K. Fuchs, I. O. Nyambok, J. D. Obel, and D. Riaroh (1997), The KRISP 94 lithospheric investigation of southern Kenya: The experiments and their main results, *Tectonophysics*, *278*, 121–147.
- Rabinowitz, P. D., M. F. Coffin, and D. Falvey (1983), The separation of Madagascar and Africa, *Science*, *220*, 67–69.
- Reeves, C. V., F. M. Karanja, I. N. MacLeod (1987), Geophysical evidence for a failed Jurassic rift and triple junction in Kenya, *Earth Planet. Sci. Lett.*, *81*, 299–311, doi:10.1016/0012-821X(87)90166-X.
- Reeves, C. (2014), The position of Madagascar within Gondwana and its movements during Gondwana dispersal, *J. Afr. Earth Sci.*, *94*, 45–57.
- Reeves, C., and M. J. De Wit (2000), Making ends meet in Gondwana: Retracing the transforms of the Indian Ocean and reconnecting continental shear zones, *Terra Nova*, *12*, 272–280.
- Reston, T. J. (2009), The structure, evolution and symmetry of the magma-poor rifted margins of the North and Central Atlantic: A synthesis, *Tectonophysics*, *468*, 6–27.
- Reston, T. J., C. R. Ranero, O. Ruoff, M. Perez-Gussinye, and J. J. Dañobeitia (2004), Geometry of extensional faults developed at slow-spreading centres from pre-stack depth migration of seismic reflection data in the Central Atlantic (Canary Basin), *Geophys. J. Int.*, *159*, 591–606.
- Rodger, M., A. B. Watts, C. J. Greenroyd, C. Peirce, and R. W. Hobbs (2006), Evidence for unusually thin oceanic crust and strong mantle beneath the Amazon Fan, *Geology*, *34*, 1081–1084.
- Salman, G., and I. Abdula (1995), Development of the Mozambique and Ruvuma sedimentary basins, offshore Mozambique, *Sediment. Geol.*, *96*, 7–41.
- Sandwell, D. T. (1984), Thermomechanical evolution of oceanic fracture zones, *J. Geophys. Res.*, *89*, 11,401–11,413.
- Sandwell, D. T., R. D. Müller, W. H. F. Smith, E. Garcia, and R. Francis (2014), New global marine gravity model from CryoSat-2 and Jason-1 reveals buried tectonic structure, *Science*, *346*, 65–67.
- Saria, E., E. Calais, D. S. Stamps, D. Delvaux, and C. J. H. Hartnady (2014), Present-day kinematics of the East African Rift, *J. Geophys. Res. Solid Earth*, *119*, 3584–3600, doi:10.1002/2013JB010901.
- Scrutton, R. A., W. B. Heptonstall, and J. H. Peacock (1981), Constraints on the motion of Madagascar with respect to Africa, *Mar. Geol.*, *43*, 1–20.
- Ségoufin, J., and P. Patriat (1980), Existence d'anomalies mésozoïques dans le bassin de Somalie. Implications pour les relations Afrique-Antarctique-Madagascar, *C. R. Acad. Sci.*, *291*, 85–88.
- Seton, M., et al. (2012), Global continental and ocean basin reconstructions since 200 Ma, *Earth-Science Reviews*, *113*, 212–270. [Available at <http://dx.doi.org/10.1016/j.earscirev.2012.03.002>.]
- Smelror, M., R. M. Key, R. A. Smith, and F. Njange (2008), Late Jurassic and Cretaceous Palynostratigraphy of the Onshore Rovuma Basin, Northern Mozambique, *Palynology*, *32*, 63–76.
- Smith, A. G., and A. Hallam (1970), The fit of the southern continents, *Nature*, *225*, 139–144.
- Soto, M., E. Morales, G. Veroslavsky, H. de Santa Ana, N. Ucha, and P. Rodríguez (2011), The continental margin of Uruguay: Crustal architecture and segmentation, *Mar. Pet. Geol.*, *28*, 1676–1689.
- Storey, M., J. J. Mahoney, A. D. Saunders, R. A. Duncan, S. P. Kelley, and M. F. Coffin (1995), Timing of hot spot-related volcanism and the breakup of Madagascar and India, *Science*, *267*, 852–855.

- Sutra, E., and G. Manatschal (2012), How does the continental crust thin in a hyperextended rifted margin? Insights from the Iberia margin, *Geology*, *40*, 139–142.
- Trompette, R. (2000), Gondwana evolution; its assembly at around 600 Ma, *C. R. Acad. Sci.*, *330*, 305–315.
- Tugend, J., G. Manatschal, N. J. Kusznir and E. Masini (2015), Characterizing and identifying structural domains at rifted continental margins: application to the Bay of Biscay margins and its Western Pyrenean fossil remnants, *Geol. Soc. London Spec. Publ.*, *413*, 171–203, doi:10.1144/SP413.3.
- Van Hinsbergen, D. J. J., S. J. H. Buitter, T. H. Torsvik, C. Gaina, and S. J. Webb (2011), The formation and evolution of Africa from the Archaean to Present: Introduction, *Geol. Soc. Spec. Publ.*, *357*, 1–8.
- Walcott, R. I. (1972), Gravity, flexure, and the growth of sedimentary basins at a continental edge, *Geol. Soc. Am. Bull.*, *83*, 1845–1848.
- Watts, A. B., and J. Stewart (1998), Gravity anomalies and segmentation of the continental margin offshore West Africa, *Earth Planet. Sci. Lett.*, *156*, 239–252.
- White, N., M. Thompson, and T. Barwise (2003), Understanding the thermal evolution of deep-water continental margins, *Nature*, *426*, 334–343.
- White, R. S., D. McKenzie, R. K. O’Nions (1992), Oceanic crustal thickness from seismic measurements and rare earth element inversions, *J. Geophys. Res.*, *97*, 19,683–19,715.
- Whittaker, J. M., A. Goncharov, S. E. Williams, R. D. Müller, and G. Leitchenkov (2013), Global sediment thickness data set updated for the Australian-Antarctic Southern Ocean, *Geochem. Geophys. Geosyst.*, *14*, 3297–3305, doi:10.1002/ggge.20181.
- Williams, S. E., D. R. Müller, T. C. W. Landgrebe, and J. M. Whittaker (2012), An open-source software environment for visualizing and refining plate tectonic reconstructions using high-resolution geological and geophysical data sets, *GSA Today*, *22*, p 4–9, doi:10.1130/GSATG139A.110.1130/GSATG139A.1
- Windley, B. F., A. Razafiniparany, T. Razakamanana, and D. Ackermann (1994), Tectonic framework of the Precambrian of Madagascar and its Gondwana connections: A review and reappraisal, *Geol. Rundsch.*, *83*, 642–659.
- Yuan, B., W. Xie., G. Liu., and C. Zhang (2012), Gravity field and tectonic features of Block L2 in the Lamu basin, Kenya, *Geophys. Prospect.*, *60*, 161–178, doi:10.1111/j.1365-2478.2011.00961.x.
- Ziegler, P. A., and S. Cloetingh (2004), Dynamic processes controlling evolution of rifted basins, *Earth Sci. Rev.*, *64*, 1–50.